JOURNAL OF MATERIALS SCIENCE **33** (1998) 5843–5847

Growth of fullerene nanoparticles prepared by the gas-evaporation technique

T. OHNO
Department of Fundamental Science, Gifu National College of Technology, Gifu 501-0495, Japan
E-mail: ohno@gifu-nct.ac.jp

S. YATSUYA
2360 Stillwater Avenue No. 308, Maplewood, MN 55119, USA

C_{60} and C_{70} fullerene nanoparticles prepared by evaporating their powders in inert gas were investigated by electron microscopy and X-ray diffraction. Crystal structures of the particles were face centred cubic (fcc) which is a stable phase at high temperature, with lattice parameters of $a = 1.42$ nm for C_{60} and $a = 1.499$ nm for C_{70}. Nanoparticles with definite crystal habits were sometimes observed among those with irregular ones. For the C_{70} nanoparticles, the higher the source temperature was, the better-defined the crystal habits were.

1. Introduction

The discovery of a method of producing large amounts of fullerenes [1] has promoted experimental and theoretical studies on them. The crystal structure of C_{60} single crystals a few millimetres in size grown from their vapour was face centred cubic (fcc) [2, 3], while for C_{70} single crystals grown from their vapour, five different phases [fcc, rhombohedral, ideal hexagonal close packed (hcp), deformed hcp and monoclinic phases from high to low temperature] were observed [4]. Green *et al.* [5] reported that on sublimation, solvent free C_{70} crystallized in a hcp1 phase, with small admixture of a hcp2 phase as well as a fcc phase. It was pointed out [4, 6] that the crystal structures of C_{70} depended strongly on thermal treatment. On the other hand, for C_{60} nanoparticles prepared by arc-discharge with amorphous carbon rods in inert gas (the so-called gas-evaporation technique), X-ray and electron diffraction patterns did not show (2 0 0) and (3 1 1) reflections [7], which are usually observed for fcc crystallites.

In this study, crystal structures and habits of C_{60} and C_{70} fullerene nanoparticles prepared by evaporating their powders in inert gas were investigated by electron microscopy and X-ray diffraction. They are discussed in relation to both growth temperature and the three growth zones of smoke, where thermal equilibrium-shaped particles of the largest size grow in the intermediate zone [8–11].

2. Experimental procedure

The work chamber used in this experiment was 210 mm in diameter and 400 mm in height. The experimental procedures for the preparation of fullerene nanoparticles were the same as described in [8, 9]. The purity of the starting powder materials (Texas Fullerenes Corp.) was 99.9% for C_{60} and 99% for C_{70}. Evaporation was carried out in most cases from a tungsten boat ($6 \times 80 \times 0.1\ mm^3$) heated up to a temperature, T_s, ranging from 1000 to 1300 °C in an argon atmosphere at a pressure, P_{Ar}, ranging from 0.7 to 2.6 kPa. In order to investigate the effect of evaporation temperature on the crystal structure and habit of C_{70} nanoparticles, C_{70} powder material was evaporated from a tantalum boat, which was covered with a tantalum sheet with two pinholes, heated up to $T_s = 1750$ °C. The specimens for electron microscopy were collected for about 1 s at various lateral distances, L, from the smoke centre at a vertical distance, V, from the boat, using the device described in [9].

Structural and morphological observations of the nanoparticles were carried out in both bright and dark field images using a JEM-100S transmission electron microscope equipped with a double tilting stage. Lattice images of C_{60} nanoparticles were taken by a transmission electron microscope operating at 300 kV. C_{70} nanoparticles of large size were observed with a scanning electron microscope (SEM). Lattice parameters of the C_{60} or C_{70} nanoparticles collected from the inner wall of the work chamber were examined by X-ray diffraction.

3. Results and discussion

3.1. General features and crystal structures of C_{60} nanoparticles

Fig. 1 shows smoke consisting of C_{60} nanoparticles prepared by evaporating C_{60} powder in an argon atmosphere at a pressure of 1.3 kPa. The nanoparticulate smoke was shaped like a candle flame, as was observed for typical metal smoke [8–11]. The smoke is, therefore, expected to consist of three growth zones. Fig. 2 shows electron micrographs of C_{60} nanoparticles collected at three growth zones on a transverse cross-section of the

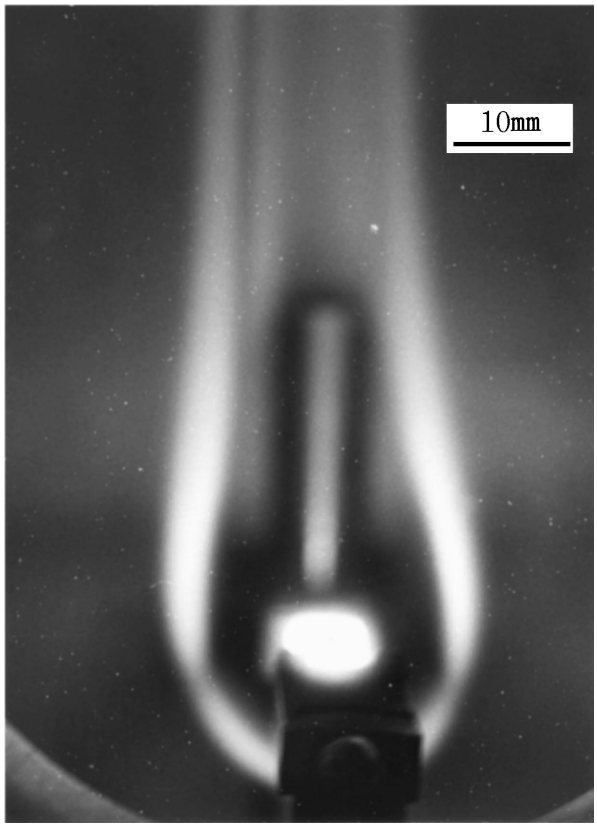

Figure 1 Smoke consisting of C_{60} nanoparticles (P_{Ar} = 1.3 kPa and T_s = 1300 °C).

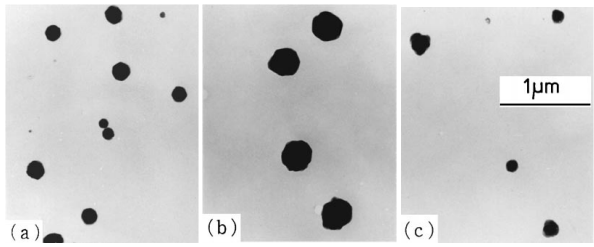

Figure 2 C_{60} nanoparticles grown at L = 0 mm (a), 3 mm (b) and 6 mm (c) on a transverse cross-section of smoke. (a), (b) and (c) correspond to the inner, intermediate and outer zones, respectively (P_{Ar} = 1.6 kPa, T_s = 1030 °C and V = 45 mm).

smoke: (a), (b) and (c) correspond to the inner, intermediate and outer zones, respectively. The particle size is largest for the particles grown in the intermediate zone. Almost all of the nanoparticles show irregular external shapes and the particle size ranges from 100 to 400 nm. It is worth noting that variation of the nanoparticles in size and external shape at the three growth zones was smaller than that of metal smoke particles [8–11]. The result is attributed to the low thermal conductivity (0.4 W mK^{-1}) of C_{60} at room temperature [12] in comparison with that of metal (for example, 400 W mK^{-1} for Cu). The C_{60} vapour, which flows outwards from its source by diffusion through the atmosphere gas, is cooled by a convection current. The outer part of the vapour zone is, therefore, cooled more rapidly than the inner part of the vapour zone [11]. But this does not produce a high gradient in vapour concentration near the vapour source, because the difference in the cooling rate of the nanoparticles at the three growth zones is small

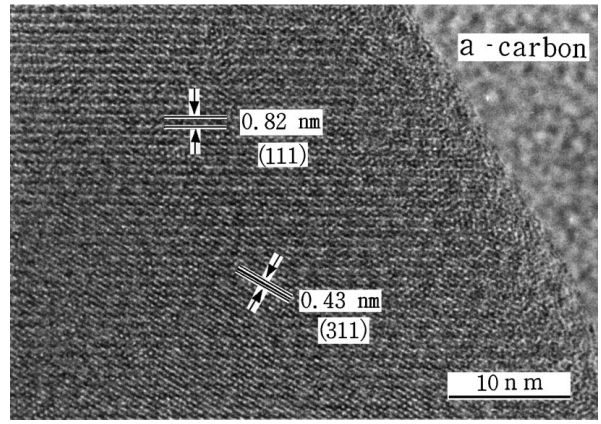

Figure 3 High-resolution electron micrograph of a C_{60} nanoparticle (P_{Ar} = 1.6 kPa, T_s = 1030 °C and V = 45 mm).

due to the low thermal conductivity of C_{60}. The low vapour concentration gradient results in a small variation in size and external shape of the nanoparticles at the three growth zones.

The powder X-ray diffraction pattern for the C_{60} nanoparticles showed four strong Bragg reflections with d spacings of 0.827, 0.504, 0.428 and 0.401 nm, each of which corresponds to {1 1 1}, {2 2 0}, {3 1 1} and {2 2 2} planes of the fcc structure, with a lattice parameter of a = 1.42 nm. The {2 0 0} reflection was absent, as was reported in the reference [7]. The absence of a {2 0 0} reflection for the C_{60} crystallite is attributed to high-speed rotation of the C_{60} molecules at the lattice points [7]. The electron diffraction pattern for the nanoparticles as well as the X-ray diffraction pattern did also show the {3 1 1} reflection, although it was reported [7] that the {3 1 1} reflection was absent in electron and X-ray diffraction patterns for C_{60} nanoparticles prepared by evaporating an amorphous carbon rod in inert gas. A high-resolution electron micrograph of the C_{60} nanoparticle is shown in Fig. 3, where the lattice image of the (3 1 1) planes is clearly observed over the wide region of the particle. The crossed lattice image shows that the particle is in the cubic phase. The presence of a {3 1 1} lattice image over the wide region of the nanoparticles prepared in this experiment implies that they were better crystallized and, therefore, contained less stacking disorder [13].

3.2. Crystal structures of C_{70} nanoparticles

The general features of C_{70} nanoparticles were almost the same as those of C_{60}. Fig. 4 shows an electron micrograph (a) of the C_{70} nanoparticles and the corresponding electron diffraction pattern (b), where the reflections are indexed with fcc structure, the {2 0 0} reflection also being absent. The powder X-ray diffraction pattern for the C_{70} nanoparticles showed seven Bragg reflections. The interplanar spacings obtained from the reflections are summarized in Table I, where they are compared with both those of C_{70} powder indexed with an fcc structure of a = 1.496 nm [5] and those of a C_{70} single crystal indexed with hcp1 structure of a = 1.0734 nm and c = 2.0276 nm [3]. Judging from the results mentioned above, the crystal structure of the C_{70} nanoparticles

TABLE I Interplanar spacings (nanometres) obtained from powder X-ray diffraction of C_{70} nanoparticles, in comparison with those of C_{70} powder indexed with fcc structure of $a = 1.496$ nm [5] and those of a C_{70} single crystal indexed with a hcpl structure of $a = 1.0734$ nm and $c = 2.0276$ nm [3]

Present study		fcc ($a = 1.496$ nm)			hcp1 ($a = 1.0734$ nm, $c = 2.0276$ nm)		
d_{obs}	I/I_0[a]	$h\,k\,l$	d_{calc}	d_{obs} (powder)	$h\,k\cdot l$	d_{calc}	d_{obs} (single)
					10.0	0.9296	0.9241
0.8715	62	111	0.8637	0.845	10.1	0.8450	
0.5308	100	220	0.5289	0.523	11.0	0.5367	
					00.4	0.5069	0.5069
					20.0	0.4648	0.4635
0.4513	92	311	0.4511	0.446	20.1	0.4530	
0.4328	23	222	0.4319	0.427	20.2	0.4225	
0.3349	37	420	0.3345	0.332	21.2	0.3320	
0.3048	25	422	0.3054		30.0	0.3099	0.3095
0.2879	16	333	0.2879		40.0	0.2324	0.2323

[a] I/I_0 is the intensity.

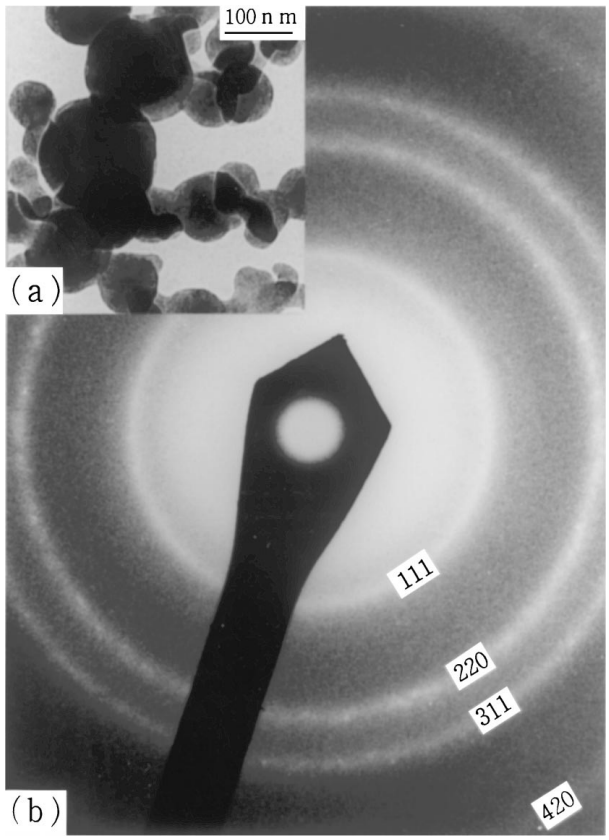

Figure 4 Electron micrograph (a) and electron diffraction pattern (b) for C_{70} nanoparticles ($P_{Ar} = 1.3$ kPa, $T_s = 1110\,^{\circ}$C and $V = 40$ mm).

grown here was found to be fcc, with a lattice parameter of $a = 1.499$ nm.

The crystal structure of the C_{70} nanoparticles grown in this experiment was fcc, as was the crystal structure of the C_{60} ones. Since the crystal structure of C_{60} fullerene is known to be fcc at a temperature higher than 260 K [14], growth of C_{60} nanoparticles with fcc structure is reasonable. But growth of C_{70} nanoparticles with fcc structure is inconsistent with that of millimetre-sized single C_{70} crystals with hcp1 structure [2, 3]. This disagreement is attributed to the different preparation methods employed, especially the different growth temperatures; the former were prepared by the gas-evaporation technique, while the latter were prepared by vapour transport at a temperature ranging from 500 to 620 °C. At a temperature higher than 345 K, the stable crystal structure of C_{70} fullerene is fcc, while hcp1 and hcp2 phases of C_{70} fullerene are metastable [4, 6]. Inferring from temperature distribution curves around a heater used in the gas-evaporation technique [15], the growth temperature of C_{70} smoke nanoparticles ranges from 200 to 300 °C (473 and 573 K, respectively) at a position $V = 2$ cm from the source at $T_s = 1200\,^{\circ}$C. Thus, C_{70} nanoparticles with fcc structure, not hcp structure, grew at the growth temperature in this experiment.

3.3. Morphology of C_{60} and C_{70} nanoparticles

Nanoparticles with definite crystal habits were sometimes observed among those with irregular ones. Fig. 5 shows a C_{60} nanoparticle with flat surfaces. The electron diffraction pattern (c) gives a [1 0 0] incidence for the fcc structure. Four {2 0 0} reflections are present, the intensity being weak [7]. All four {2 2 0} reflections are split due to refraction effect at the edges of the particle. The dark field image (b) taken with 0 2 2 reflection indicates that the particle is a single crystallite with a planar defect. The crystal habit is found from the above observation to be a octahedron truncated by {1 0 0} planes, which is known to be a thermal equilibrium crystal habit characteristic of fcc metal nanoparticles grown in the intermediate zone of smoke [11].

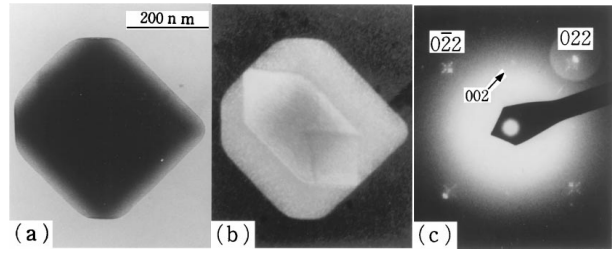

Figure 5 A C_{60} nanoparticle showing the crystal habit of a octahedron truncated by {1 0 0} planes. (a) Bright field image, (b) dark field image taken with 0 2 2 reflection and (c) electron diffraction pattern showing [1 0 0] incidence for fcc structure ($P_{Ar} = 1.6$ kPa, $T_s = 1030\,^{\circ}$C and $V = 45$ mm).

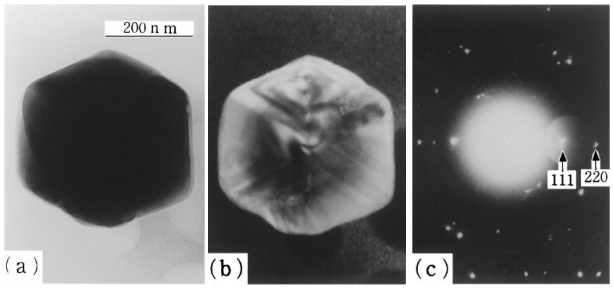

Figure 6 A C_{60} multiply twinned nanoparticle. (a) Bright field image, (b) dark field image taken with 1 1 1 reflection and (c) electron diffraction pattern ($P_{Ar} = 1.6$ kPa, $T_s = 1030\,^{\circ}$C and $V = 45$ mm).

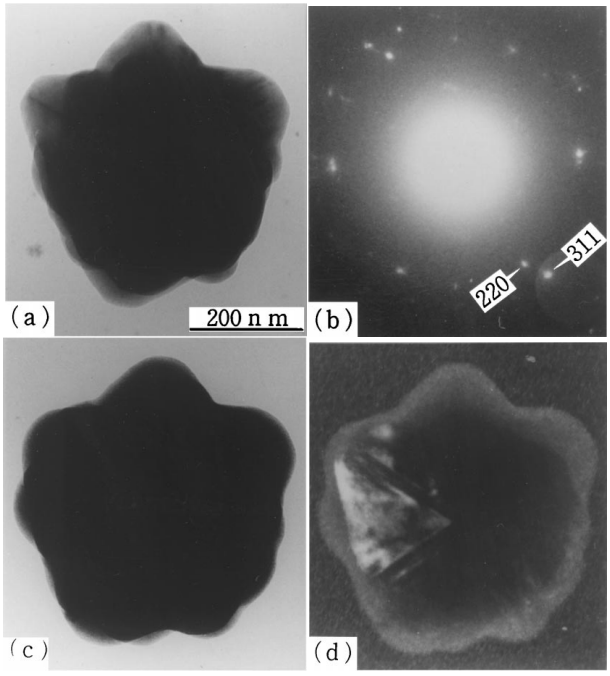

Figure 7 A C_{70} multiply twinned nanoparticle. (a) Bright field image, (b) electron diffraction pattern. The electron micrographs (c) and (d) were taken for the particle tilted by 20° against that of (a). The dark field image (d) was taken with 2 2 0 reflection ($P_{Ar} = 2.6$ kPa, $T_s = 1250\,^{\circ}$C and $V = 50$ mm).

Fig. 6 shows a C_{60} nanoparticle with the external shape of a hexagonal polyhedron. The dark field image (b) taken with 1 1 1 reflection gives a contrast showing that it is a multiply twinned particle, characteristic of smoke particles of fcc metals [11].

Fig. 7 shows a horned C_{70} nanoparticle, which was grown at a considerably higher source temperature. The electron micrographs (c) and (d) were taken for the particle tilted by 20° against that of (a). The electron diffraction pattern (b) corresponding to the image (a) suggests the particle contains planar defects in it. From the dark field image (d) taken with 2 2 0 reflection, it is also found to be a multiply twinned particle. A SEM micrograph of a C_{70} nanoparticle with many horns, which was also grown at a considerably higher source temperature, is shown in Fig. 8. These crystal habits were observed for both C_{60} and C_{70} nanoparticles grown from a source heated up to a temperature higher than 1200 °C.

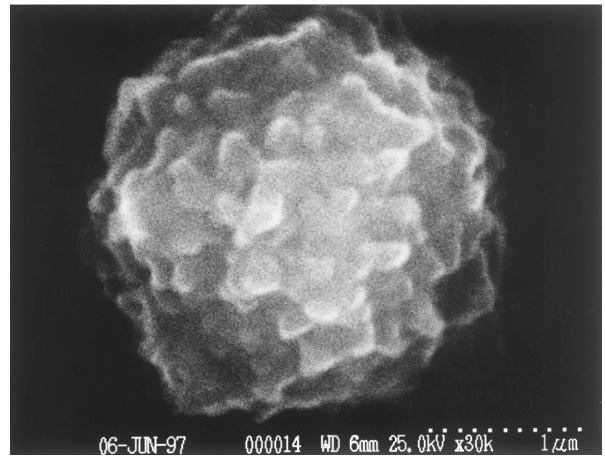

Figure 8 A SEM micrograph of a C_{70} nanoparticle with many horns ($P_{Ar} = 2.6$ kPa, $T_s = 1230\,^{\circ}$C and $V = 50$ mm).

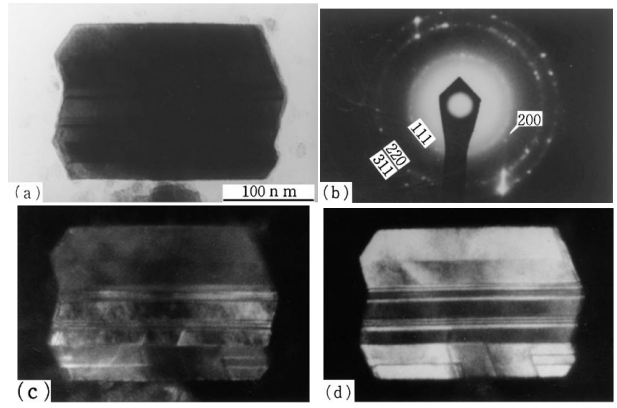

Figure 9 A C_{70} twinned nanoparticle grown at a high source temperature. (a) Bright field image, (b) electron diffraction pattern, and (c) and (d) dark field images taken with 2 2 0 and 3 1 1 reflections, respectively ($P_{Ar} = 1.3$ kPa, $T_s = 1750\,^{\circ}$C and $V = 30$ mm).

The horned shapes observed in this experiment reflect vapour growth in the high vapour densities of fullerene C_{60} or C_{70}, since the vapour pressures at a temperature higher than 1200 °C are high enough (about 2 Pa for C_{60} and about 1 Pa for C_{70} at 600 °C [16]) for nanoparticles to grow in the vapour phase.

When the source temperature was above 1750 °C, C_{70} nanoparticles with definite crystal habits (for example with external shapes of triangular plates or hexagonal columns) were always found among those with irregular external shapes. These well defined habits are due to the high growth temperature. Fig. 9 shows a C_{70} nanoparticle grown at $T_s = 1750\,^{\circ}$C. The bright field image (a) shows a definite habit. The electron diffraction pattern (b), which also reveals weak {2 0 0} reflections, shows straight streaks. The contrast in the dark field images (c) and (d) taken with 2 2 0 and 3 1 1 reflections, respectively, is the reverse. The particle is, therefore, found to contain many planar defects parallel to each other. These planar defects imply that the growth of the particle was achieved by transformation to a fcc phase after formation of a metastable hcp phase at a high temperature.

4. Conclusions

C_{60} and C_{70} fullerene nanoparticles prepared by evaporating their powders in inert gas were investigated by electron microscopy and X-ray diffraction. The crystal structure of C_{60} nanoparticles was fcc, with lattice parameters of $a = 1.42$ nm in accordance with the results already reported. It was found in this experiment that the crystal structure of C_{70} nanoparticles was also fcc, which is a stable phase at high temperature, with lattice parameters of $a = 1.499$ nm. The disagreement in the crystal structure of single C_{70} crystals a few millimetres in size is attributed to the different preparation methods, especially the different growth temperatures.

C_{60} nanoparticles with definite crystal habits characteristic of fcc metal nanoparticles were sometimes observed among those with irregular ones. For the C_{70} nanoparticles, the higher the source temperature was, the better-defined the crystal habits were. The growth of well defined C_{70} nanoparticle was inferred to be achieved by the transformation to a fcc phase after formation of a metastable hcp phase at high temperature. The horned shapes for the C_{60} or C_{70} nanoparticles observed in this experiment reflect vapour growth in the high vapour densities of fullerene C_{60} or C_{70}.

Acknowledgements

The authors thank Dr Hayashi in NTT for his useful suggestions and also thank Mr Yamada, Mr Shiraki and Mr Mori, the graduates of Gifu National College of Technology for their assistance. This work was partly supported by a Grant-in-Aid for Scientific Research (No. 08 650 027) from the Japan Ministry of Education, Science and Culture.

References

1. W. KRÄTSCHMER, L. D. LAMB, K. FOSTIROPOULOS and D. R. HUFFMAN, *Nature* **347** (1990) 354.
2. J. LI, T. MITSUKI, M. OZAWA, H. HORIUCHI, K. KISHIO, K. KITAZAWA, K. KIKUCHI and Y. ACHIBA, *J. Cryst. Growth* **143** (1994) 58.
3. J.-B. SHI, W.-Y. CHANG, S.-R, SU and M.-W. LEE, *Jpn. J. Appl. Phys.* **35** (1996) L45.
4. M. A. VERHEIJIEN, H. MEEKES, G. MEIJER, P. BENNEMA, J. L. DE BOER, S. VAN SMAALEN, G. VAN TENDELOO, S. AMELINCKS, S. MUTO and J. VAN LANDUYT, *Chem. Phys.* **166** (1992) 287.
5. M. A. GREEN, M. KURMOO, P. DAY and K. KIKUCHI, *J. Chem. Soc. Chem. Commun.* (1992) 1676.
6. G. B. M. VAUGAHAN, P. A. HEINEY, D. E. COX, J. E. FISCHER, A. R. MCGHIE, A. L. SMITH, R. M. STRONGIN, M. A. CICHY and A. B. SMITH III, *Chem. Phys.* **178** (1993) 599.
7. C. KAITO, S. KIMURA, T. SAKAMOTO, Y. YOSHIMURA, R. KAIGAWA, T. SAKAGUCHI, Y. NAKAYAMA and Y. SAITO, *J. Cryst. Growth* **134** (1993) 157.
8. S. YATSUYA, S. KASUKABE and R. UYEDA, *Jpn. J. Appl. Phys.* **12** (1973) 1675.
9. T. OHNO and K. YAMAUCHI, *ibid.* **20** (1981) 1385.
10. T. OHNO, S. YATSUYA and R. UYEDA, *ibid.* **15** (1976) 1213.
11. T. HAYASHI, T. OHNO, S. YATSUYA and R. UYEDA, *ibid.* **16** (1977) 705.
12. R.-C. YU, N. H. TEA, M. B. SALAMON, D. C. LORENTS and R. MALHORTA, *Phys. Rev. Lett.* **68** (1992) 2050.
13. R. L. MENG, D. RAMIREZ, X. JIANG, P. C. CHOW, C. DIAZ, K. MATSUISHI, S. C. MOSS, P. H. HOR and C. W. CHU, *Appl. Phys. Lett.* **59** (1991) 3402.
14. W. I. F. DAVID, R. M. IBBERSON and T. TATSUO, *Proc. R. Soc. Lond. A* **442** (1993) 129.
15. C. KAITO and K. FUJITA, *Jpn. J. Appl. Phys.* **25** (1986) 496.
16. J. ABREFAH, D. R. OLANDER, M. BALOOCH and W. J. SIEKHAUS, *Appl. Phys. Lett.* **60** (1992) 1313.

Received 9 July 1997
and accepted 30 July 1998